World Academy of Science, Engineering and Technology
International Journal of Mechanical and Mechatronics Engineering
Vol:7, No:6, 2013

Conceptual Design and Characterization of Contractile Water Jet Thruster Using IPMC Actuator

Muhammad Farid Shaari and Zahurin Samad

Open Science Index, Mechanical and Mechatronics Engineering Vol:7, No:6, 2013 publications.waset.org/12518/pdf

***Abstract*—**This paper presents the design, development and characterization of contractile water jet thruster (CWJT) for mini underwater robot. Instead of electric motor, this CWJT utilizes the Ionic Polymer Metal Composite (IPMC) as the actuator to generate the water jet. The main focus of this paper is to analyze the conceptual design of the proposed CWJT which would determine the thrust force value, jet flow behavior and actuator's stress. Those thrust force and jet flow studies were carried out using Matlab/Simscape simulation software. The actuator stress had been analyzed using COSMOS simulation software. The results showed that there was no significant change for jet velocity at variable cross sectional nozzle area. However, a significant change was detected for jet velocity at different nozzle cross sectional area ratio which was up to 37%. The generated thrust force has proportional relation to the nozzle cross sectional area.

***Keywords*—**Contractile water jet thruster, IPMC actuator, Thrust force.

I. Introduction

ONE of the vital factor in designing an underwater vehicle or robot is the determination of the propulsion system which has the ample thrust force range to overcome the drag with good thrust efficiency. Contractile water jet thruster (CWJT) is an alternative propulsion method especially for small scale underwater robot. The significant differences of this contractile thruster relatively compared to other typical water jet thruster are the deformable pressure chamber volume during and the utilization of alternative actuator instead of electric motor [1]. There are few types of actuators that could be utilized for the contraction mechanism which are electrical motor, smart material actuator and electromagnetic actuation device [2], [3]. In this research, two lateral Ionic Polymer Metal Composite (IPMC) smart material had been selected as the actuator. The advantages of using IPMC actuator are including the low voltage consumption, high and fast displacement, able to work in the water and quite in operation [4]. Generally there are two states of operation which are the inflation and deflation phase. In the inflation phase, the CWJT volume increased, reducing the pressure and drawing in the water. This stage is followed by deflation contraction process whereby the IPMC actuator bend inward to reduce the CWJT volume, increase the internal pressure and jetting out the water through nozzle. Unlike the typical fixed body water jet thruster, the deformable volume has variable parameters such as volume, mass flow rate and pressure differentiation which are difficult to measure especially in a small scale dimension. Thus, in order to determine the CWJT specification and its possible performance, we had characterized the CWJT using simulation software prior to do experimental works. In the investigation, we had focused on the thrust force generation, jet flow behavior and the stress of the IPMC actuator. Model and simulation process had been worked out using MATLAB/Simscape simulation software to observe the fluid flow rate and pressure in the designed system. Stress analysis had been completed using COSMOS simulation software.

The conceptual design of the CWJT will be discussed further in detail in Section II. Section III justified the specific system dynamic model and the related simulation analysis. Finally in Section IV, the results of the analysis are presented and discussed.

Muhammad F. Shaari is a lecturer at the Faculty of Mechanical and Manufacturing Engineering, Universiti Tun Hussein Onn Malaysia, 86400 Parit Raja, Batu Pahat, Johor, Malaysia. Currently, he is pursuing his PhD study at School of Mechanical Engineering, University Sains Malaysia, Penang, Malaysia. (phone: 607-453 7654, fax: 607-453 6080, e-mail: mdfarid@uthm.edu.my).

Z. Samad is an Associate Professor at School of Mechanical Engineering, University Sains Malaysia, Seri Ampangan, 14300 Nibong Tebal, Penang, Malaysia (e-mail: zahurin@eng.usm.my).

II. Conceptual Design

A. Overall Design

Basically, the CWJT is consists of four main parts which are the inlet, lateral actuator, pressure chamber and nozzle (Fig. 1). The selected design was based on boxed shape thruster with overall dimension of 70mm x 40mm x 10mm (LxWxT). Working as a single thruster, this CWJT will be attached under the hull which accommodates the battery, controller and driving circuit (Fig. 2). The front inlet opening has diffuser design with 5˚ degree divergent angle to acquire valveless effect [5]. The application of the valveless design selected to avoid the additional disturbance which would come from the single flow valve. Meanwhile the nozzle had diffuser design too but the cross sectional area ratio of the nozzle was not fixed at certain degree for simulation purpose.

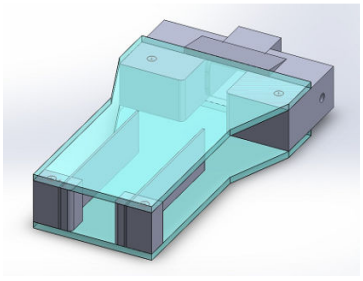


Fig. 1 Isometric view of the IPMC actuated CWJT

Open Science Index, Mechanical and Mechatronics Engineering Vol:7, No:6, 2013 publications.waset.org/12518/pdf

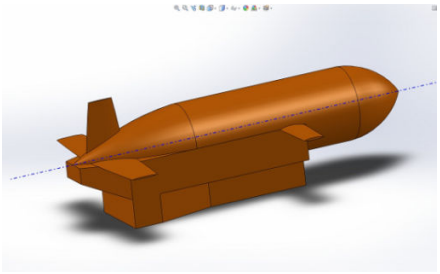


Fig. 2 CWJT location under the main hull

B. Water jet Propulsion System

Water jet propulsion system was modeled from the thrust force, T_f equation which was derived from momentum equation, (1). In the CWJT case, the volume variation in the pressure chamber during inflation and deflation process results different mass volume at different rate entering and leaving the pressure chamber. Thus, for (1) the mass should be considered as mass flow rate, $\dot{m}$ instead of fixed solid mass (2). Replacing (2) into (1) becomes (3).

$$T_f = ma = m\frac{dv}{dt} \tag{1}$$

$$\dot{m} = \frac{\Delta m}{dt} = \rho A v = \rho Q \tag{2}$$

$$T_f = \rho Q \frac{dv}{dt} \tag{3}$$

where $\dot{m}$ is the mass flow rate, ρ is the water density, A is the cross sectional at the nozzle, Q is the jet flow rate and v is the velocity of the fluid. The value of $\dot{m}$ is essential to determine the thrust force which is the referred as momentum changes during the contraction of the pressure chamber.

C. Actuator Design the Control System

The proposed CWJT had two lateral IPMC actuators. IPMC is a polymer with plated metal ions at both of its surface and becomes the polarity to the actuator [4]. The mobile cation in the IPMC manage to combine with water molecules and moves to cathode polarity when an amount of voltage attached to the polarities. The accumulation of water molecules stimulates the actuator to bend towards positive polarity. Each actuator had cantilever beam shape form. If the polarity alternates at certain frequency (in the of AC voltage supply), the IPMC actuator oscillates due to the supplied frequency. The maximum displacement and bending speed depends on the length and thickness of the IPMC actuator.

The dimension of the CWJT IPMC actuator was 35mm x 5mm x 0.45mm (LxWxT). In the previous characterization experiment, the IPMC actuators drew 2-3V voltage to oscillate. For characterization analysis, function generator was utilized to produce alternating voltage with certain actuating frequency. However, as for mobile robot application, the CWJT received its signal from Arduino microcontroller. The produced signal will be amplified using amplifier which contained in the IPMC driver. Fig. 3 shows the control system configuration.

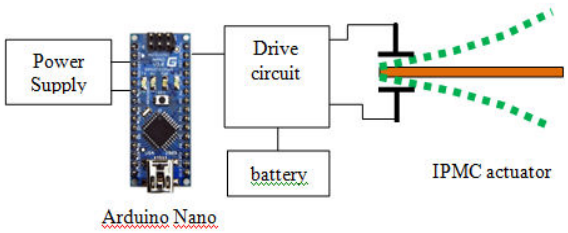


Fig. 3 Control system hardware using Arduino Nano

III. Simulation Analysis

A. Thrust Force Generation at Different Nozzle Area

The main aim of this analysis was to investigate the influence of the nozzle opening area and the nozzle area ratio on the generated thrust force. The MATLAB/Simscape Hydraulic simulation software was employed to do the simulation. This software is a MATLAB-SIMULINK based simulation software to analyze system design which involving hydraulic and fluid application. Based on (3), thrust force could be generated by having the fluid density, fluid flow rate and the change of velocity of the fluid. In this analysis, the thrust force calculation was made for the jetted out fluid from the pressure chamber via a nozzle. Therefore, in the simulation the pressure chamber was represented using 'Ideal Hydraulic Pressure Source' block (IHPS) and the nozzle was represented by 'Gradual Area Change' block. In the real application, the contractile function would not only provide differential volume change but it involves internal pressure changes too. Thus we applied sine wave block as signal source for the differential change of the pressure during inflation-deflation process. The amplitude of the sine wave was set as the estimated maximum pressure that could be achieved in the pressure chamber during contraction. The estimated pressure value was calculated from the maximum force generated by the lateral IPMC actuator (4),

$$P_{act} = \frac{\sum_{n} F_{IPMC}}{A} + \rho h g \tag{4}$$

where P_{act} is the actuating pressure, F_{IPMC} is the actuating force from IPMC actuator, A is the force targeted area, ρ is the fluid density (997.661kgm^{-3}), h is the underwater depth and g is the gravitational acceleration (9.81ms^{-2}). P_{act} was set at 26.67kg/m^2. Simulink-Physical Converter was utilized to transfer the signal data from sine wave source to the IHPS block. Hydraulic fluid was set to water and operating temperature was set to 25°C. The fluid flow rate reading was taken using the 'Ideal Hydraulic Flow rate Sensor' (IHFS) and displayed by a scope. Thrust force was calculated by entering the Q and V into (3). Nozzle opening area was changed

Open Science Index, Mechanical and Mechatronics Engineering Vol:7, No:6, 2013 publications.waset.org/12518/pdf

gradually from 25mm^2 to 400mm^2. Besides, the nozzle inlet and outlet opening area was also changed to certain ratio. The ratio was determined by percentage where the value was 10%, 20% and 30%. Figs. 4 and 5 show the definition of nozzle opening area reduction in percentage and MATLAB/Simscape block diagram of the system respectively. The jetted fluid velocity was calculated from the gained fluid flow rate.

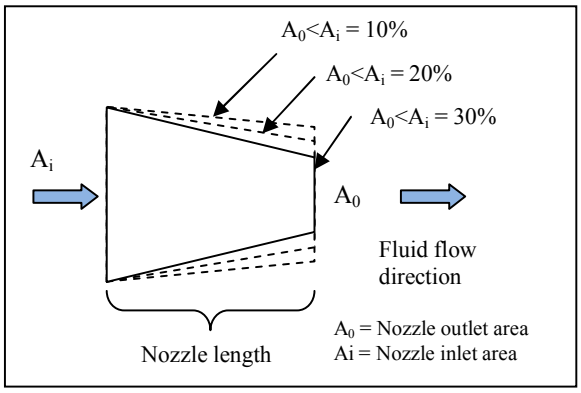


Fig. 4 Nozzle inlet and outlet area reduction in terms of percentage

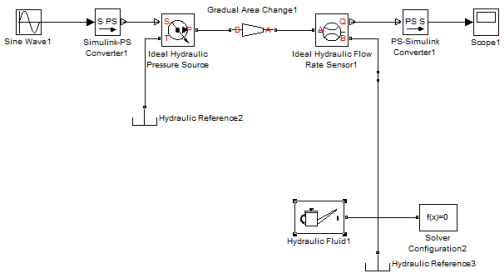


Fig. 5 MATLAB/Simscape Hydraulic Block Diagram to measure the fluid flow rate

B. Pressure Drop across the Nozzle

Pressure drop via nozzle is a significant factor in designing a water jet propulsion system. Generally, engineers try to minimize pressure drop so that the jetted pressure is higher than the surrounding pressure so it would optimize the thrust force. Equation (5) was derived as an extension to (1) and (3) to describe the pressure factor on the generated thrust force.

$$T_f = \rho Q \frac{dv}{dt} + (P_n - P_\infty) A_n \quad (5)$$

where P_n is the nozzle at the pressure, $P\,\dot{m}$ is the surrounding pressure and A_n is the nozzle opening area. In this analysis, we would like to determine how far the variation of the nozzle cross sectional area and nozzle opening area ratio would contribute to the pressure drop value. MATLAB/Simscape simulation software was employed to estimate the pressure drop value of the system. In this case, 'Ideal Hydraulic Flow rate Source' block was utilized to generate the flow rate and directly connected to a nozzle (Fig. 6). "Ideal Hydraulic Pressure Sensor' block was applied to measure the pressure drop across the nozzle. Sine wave block was utilized to generate the signal to the flow rate source. The maximum amplitude of the sine wave was referred to the maximum flow rate that could be generated by real thruster. The maximum flow rate of the real thruster was defined in the previous experiment of the IPMC actuator characterization. The nozzle area varies gradually as mentioned for fluid flow rate and jet velocity measurement.

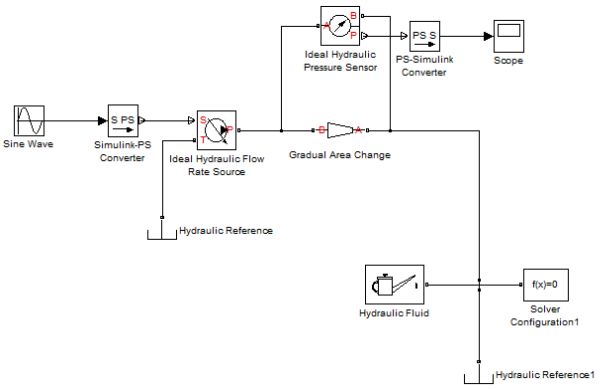


Fig. 6 MATLAB/Simscape Hydraulic Block Diagram to measure the pressure drop across the nozzle

C. Actuator's Stress Analysis

Operating at frequent oscillation for a long period would shorten the life span of the actuator. Thus, it is vital to investigate where the most stress part of the actuator is. Being clamped about 5mm at one tip and it is free at the other tip, this IPMC actuator works as a cantilever beam. The bending model in the water could be defined as (6) [6]:

$$EI\frac{\delta^4 \omega(z,t)}{\delta z^4} + C\frac{\delta \omega(z,t)}{\delta t} + \rho_m A\frac{\delta^2 \omega(z,t)}{\delta t^2} = f(z,t) \quad (6)$$

where E is the Young Modulus, I is the moment inertia, ω is the radial deflection, C is the damping ratio, ρ_m is the density, A is the cross sectional area of the actuator an $f(z,t)$ is the distribution force density acting on the IPMC actuator along the z axis. In Laplace transform, (7) becomes;

$$EI\frac{\delta^4 \omega(z,s)}{\delta z^4} + C\omega s(z,s) + \rho_m A s^2 \omega(z,s) = F(z,s) \quad (7)$$

However, according to Chen [6], the acting force on the IPMC actuator is not only from the internal water molecules movement but also from the external hydrodynamic force, $F_{hydro}(z,s)$. This hydrodynamic force can be defined as (8):

$$F_{hydro}(z,s) = -\rho_\omega \frac{\pi}{4} W^3 s^2 \Gamma_1(\omega)\omega(z,s) \quad (8)$$

where W is the width of the IPMC actuator, Γ1(ω) is the hydrodynamic function for the IPMC actuator subject to an oscillation with radial frequency, ω and ρ_ω is the fluid density. The simulation analysis was carried out using COSMOS

Open Science Index, Mechanical and Mechatronics Engineering Vol:7, No:6, 2013 publications.waset.org/12518/pdf

software.

IV. Result and Discussion

A. Thrust Force

Fig. 7 shows the volumetric flow rate of the water jet. The flow rate increases proportionally to the increment of the nozzle outlet area. This linear and proportional relation means the jet velocity has a constant value. The result also shows that wider nozzle area opening would have higher flow rate. At 400mm^2 outlet opening, it would reach the flow rate of 1.60 x 10^6 mm^{3}s^{-1}. Different inlet-outlet area of the nozzle at certain percentage presents a slightly small variation to the graphs. The nozzle with 10% changes of its inlet-outlet opening area has greater flow rate increment compared to the other two ratios.

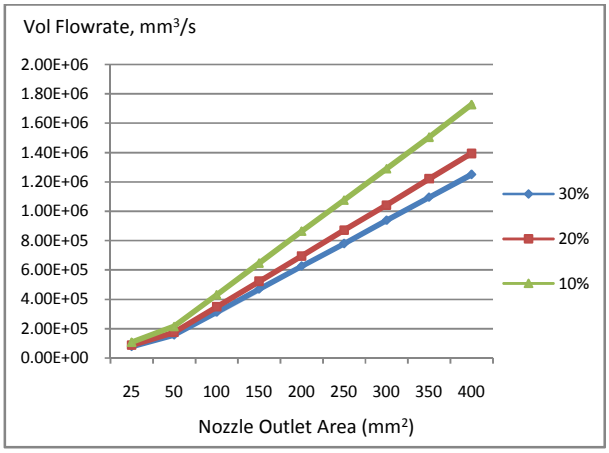


Fig. 7 Volumetric Flow rate at different nozzle area and inlet-outlet ratio

The constant value of the jet velocity at different nozzle area shows there is no significant influence of nozzle area to the jet velocity. However, obvious information of the jet velocity value comes from the different inlet-outlet area ratio of the nozzle as stated in Fig. 8. It shows that the nozzle with bigger difference in the inlet-outlet area ratio provides less velocity compared to the nozzle with less inlet-outlet area ratio. The 10% nozzle difference is relatively has almost 20% greater velocity than the 20% nozzle difference and almost 28% greater velocity than the 30% nozzle difference. The measured velocity is the estimated jet velocity for a static thruster. In addition, this velocity is not the only velocity that must be taken into account to calculate the generated thrust force. The real thruster has additional velocity vectors because the thruster is moving while producing jet to the opposite direction it is heading. Fig. 9 depicts the gained thrust force from the acquired fluid flow rate and jet velocity data. Generally the thrust force has proportionally linear relation to the nozzle area. From the graph, ideally we could conclude that bigger nozzle opening would have better thrust force, but there are few other considerations that must be concerned. In fact, thrust force is all about energy transfer from one form to another. An efficient energy transfer mechanism would have efficient propulsion. However in reality, we must consider the energy loss during the contraction either in the system or to the surrounding such as wake formation. Among the three inlet-outlet area ratio, the nozzle with lowest percentage (10%) has the highest thrust force. At 400mm^2 nozzle area, the thrust force would reach more than 7kgms^{-2}. The value of this thrust is vital to anticipate the possible dimension of the thruster and entire robot body.

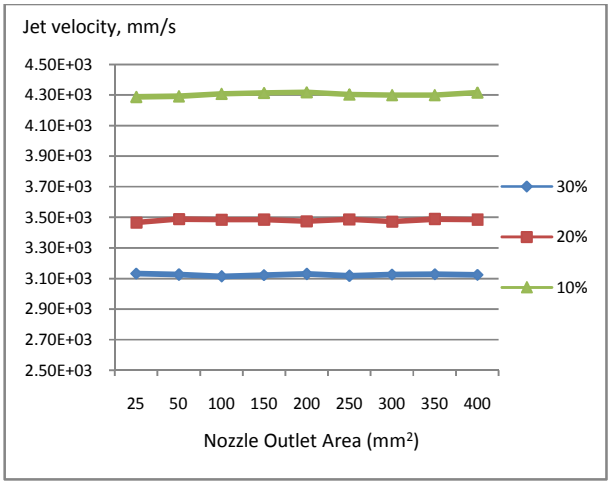


Fig. 8 Jet velocities at different nozzle area and inlet-outlet ratio

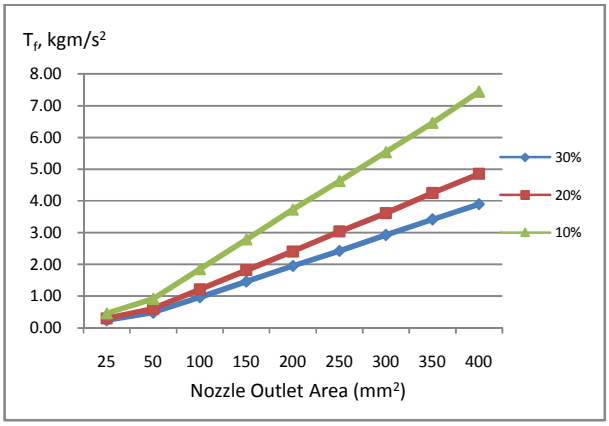


Fig. 9 Thrust Force at different nozzle area and inlet-outlet ratio

B. Pressure Drop

In Fig. 10, the graph exhibits the value of the pressure drop across the nozzle at different nozzle area. For all three inlet-outlet nozzle area ratio, the pressure drop value had been reduced tremendously between 25mm^2 and 100mm^2 nozzle area. After 100mm^2, the pressure drop almost at constant. The greatest pressure drop recorded was the nozzle with highest inlet-outlet area ratio which starts with 25 mm^2 nozzle area. Contrary to the highest ratio, the lowest inlet-outlet area ratio has the least pressure drop value.

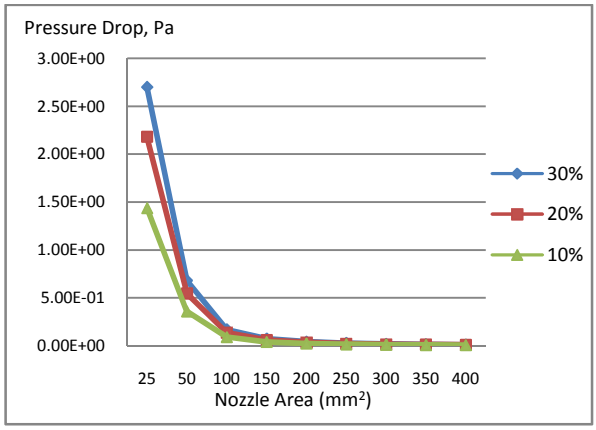


Fig. 10 Pressure drop data at different nozzle area

C. Body Stress and Strain Analysis

The simulation analysis shows that the maximum stress focused at the nearest point to the clamping zone. The Von Misses stress value was estimated at 6.564e5 Nm^{-2}. The maximum displacement of the 30mm length IPMC actuator was 9.61mm. This value is lower than its displacement in air, which was around 96% reduction. This reduction was a result from the hydrodynamic force influence. In addition to the hydrodynamic force, there is another force that had not been counted. This force comes from the compression of the water inside the pressure chamber. The small nozzle ($100mm^2$) gave another damping coefficient factor. However, the IPMC actuator was aligned such position to ensure the influencing gravitational force could be neglected. Fig. 11 shows the highest stress point to the IPMC actuator.

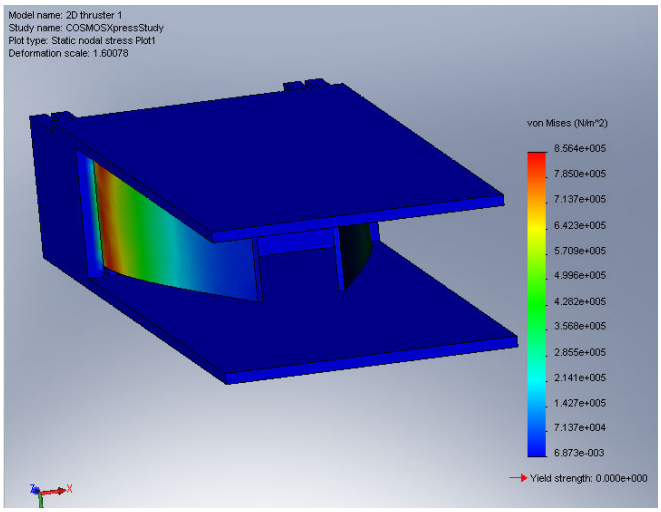


Fig. 11 Actuator stress zone

V. Conclusion

Nozzle opening area has significant influence on the generated thrust force. It has linear and proportional relation to the thrust force and the fluid flow rate. However, this trend of relation shows that the jet velocity has not being affected with the changes of nozzle area. However, the differentiation of inlet-outlet nozzle area gives significant influence to the jet velocity value. The pressure drop was great for a nozzle area which is less than $100mm^2$.

VI. Recommendations

The gained data in this research is vital for preliminary stage in designing the thruster. It is difficult to anticipate the required thrust force with complex parameter relation and few uncertainties in the constant value. Another effective work towards the development of this thruster is the implementation of optimization and design for experiment (DOE). It is suggested to have more detail model to determine the influence parameters for the designed system.

Acknowledgment

The author gratefully acknowledges support of this work by Ministry of Higher Education of Malaysia (MOHE) for their ERGS 2011 grant sponsorship, Universiti Tun Hussein Onn Malaysia for sponsoring the research fund and Universiti Sains Malaysia for their technical and facilities support.

References

[1] M.F.Shaari, Z. Samad, M.E.Abu Bakar and M. Jaafar,"Design Consideration of Bio-Inspired Water Jet Propulsor for Mini Autonomous Underwater Robot", Advanced Materials Research, vol. 463-464, 2012, pp 1583-1588.

[2] A. P. Thomas, M. Milano, M. G. G. Sell, K. Fischer, and J. Burdick: Synthetic Jet Propulsion for Small Underwater Vehicles, IEEE Int. Conf. of Robotics and Automation, 2005, pp. 181-187.

[3] M.Krieg and K.Mohseni, " Dynamic Modelling and Control of Biologically Inspired Vortex Ring Thrusters for Underwater Robot Locomotion", IEEE Trancsactions on Robotics, 2010, pp 1-13.

[4] S. Xu, B. Liu and L. Hao, "A Small Remote Operated Robotic Fish Actuated by IPMC", Proceedings of the IEEE International Conference on Robotics and Biomimetics, 2009, pp 1152-1156.

[5] E. Stemme and G. Stemme, "A Valveless Diffuse/Nozzle-based Pump", Sensors and Actuators A, vol. 39, 1993, pp.159-167.

[6] Z. Chen, S. Shatara and X. Tan, "Modelling of Biomimetic Robotic Fish Propelled by an Ionic Polymer-Metal Composite Caudal Fin", IEEE/ASME Transactions on Mechatronics, vol.15, no.3, 2010, pp 448-458.

Open Science Index, Mechanical and Mechatronics Engineering Vol:7, No:6, 2013 publications.waset.org/12518/pdf